

A Numerical Simulation of Transport Layer Thickness Effect in Tin-Based Perovskite Solar Cell

Asrul Izam Azmi¹, Muhammad Yusof Mohd Noor², Mohd Halim Irwan Ibrahim³, Fauzan Ahmad⁴, Mohd Haniff Ibrahim^{5*}

^{1,2,5} School of Electrical Engineering, Faculty of Engineering, Universiti Teknologi Malaysia, 81310 Johor, Malaysia

E-mail: hanif@fke.utm.my

³ Faculty of Mechanical and Manufacturing Engineering, Universiti Tun Hussein Onn Malaysia, Batu Pahat 86400 Johor, Malaysia

⁴ Malaysia-Japan International Institute of Technology, Universiti Teknologi Malaysia, 54100 Kuala Lumpur, Malaysia

Received: August 01, 2022

Revised: August 25, 2022

Accepted: September 02, 2022

Abstract— This paper investigates the performance of a planar n-i-p perovskite solar cells (PSC) with lead-free perovskite absorber for three different metal oxides serving as the electron transport layer (ETL). A tin (Sn) based PSCs - with i) zinc oxide (ZnO), ii) titanium oxide (TiO₂) and iii) tin oxide (SnO₂) as the ETL, and spiro-MeOTAD as the hole transport layer (HTL) - are modeled and simulated using a 1-dimensional numerical software (SCAPS 1-D). Thicknesses of both the methylammonium tin iodide (CH₃NH₃SnI₃) absorber and the ETL are varied for the purpose of achieving the optimum power conversion efficiency (PCE). For all metal oxide candidates, thickness of lead-free perovskite absorber layer is varied from 400 nm to 1500 nm. The obtained results show that the optimum recorded PCE is achieved at 900 nm. Moreover, the highest PCE value of 8.10% is observed for 80 nm thickness of SnO₂ compared to 8.05% for ZnO and 7.99% for TiO₂. Additionally, the results unveil that for a constant HTL thickness of 80 nm and ETL thickness increment up to 300 nm, the PCE is slightly reduced between 0.12% and 0.99% for all ETLs. We believe that this is the first simulation effort that evaluates the effect of transport layer thickness on the performance of lead-free PSC, hoping that the findings will be useful for the research community, particularly for those working in the field of solar cells fabrication and development.

Keywords— Perovskite solar cell; SCAPS 1-D; Hole transport layer; Electron transport layer; Power conversion efficiency.

1. INTRODUCTION

Researching for alternative energy resources has been a topic of great interest since few decades back owing to the greater exhaustion of fossil-based resources which includes coal, oil and natural gas. Apart from that, the negative impacts imposed by these resources such as emission pollutants, global warming and climate change has further steered more efforts towards alternative energy resources. Energy harvesting from the sun has been majorly attractive since its first conceptual inception in 1839 by Alexandre-Edmond Becquerel [1].

Organic-inorganic halide perovskite solar cells (PSC) is one of the emerging technologies in the current third generation of solar cell. Since its first in-lab demonstration in 2009 [2], research on PSC has been increased enormously to improve the power conversion efficiency. Starting from the work by Kojima and his co-workers [2] which yielded an efficiency of 3.8%, the latest validated efficiency for single junction PSC by National Renewable Energy Laboratory (NREL) stands at 25.7% [3]. In traditional PSC, lead (Pb) element has been used as the material for absorber layer and it has been vastly demonstrated in literature [4-7]. However, owing to the drawbacks of the Pb element that generates large

* Corresponding author

scale heavy metal pollution and causes a threat to the environment, replacement of Pb with non-toxic elements is a key success for environmental safety.

Tin (Sn) elements with a similar bandgap to Pb cations have been the most plausible choice to replace the Pb. Evidently, the incorporation of Sn elements into perovskite absorber has been demonstrated for both single junction [8-13] and multijunction/tandem solar cells [14-16]. From our review, most of these efforts have been concentrated on investigating the effect of absorption layer thickness, defect density, bandgap, interface defect layer, materials candidate for hole transport layer (HTL)/electron transport layer (ETL) and temperature effects to the solar cell performance. Note that Roy et al. [13] and Rai et al. [14] have addressed the effect of HTL thickness variation in their simulation work. They have proposed few materials as HTL and cumulative findings showed that the PSC performances were largely determined by the HTL materials and the layer thickness. However, to the best of our knowledge, the effect of the ETL thickness is yet to be explored and thus, this paper is presented to address the topic. Fundamentally, it is known that transport layers play important roles in the device structure of PSC. For instance, ETL extracts the electrons from the absorber layers and minimizes the electrons-holes recombination in PSC. Similarly, the HTL provides the driving force of charge transport and minimizes the charges recombination through its natural role as the electron blocking layer.

In this paper, we will evaluate the effect of ETL thicknesses to the PSC parameters (open-circuit voltage (V_{OC}), short-circuit current (I_{SC}), fill factor (FF) and power conversion efficiency (PCE). Primarily, a lead-free PSC model by Liangsheng et al. [10] will be used as our benchmark due to their main investigation on PSC parameters (V_{OC} , I_{SC} , FF and PCE) related to absorber layer thickness. In [10], Liangsheng et al. used solar cell capacitance simulator (SCAPS 1-D) numerical software [17], to simulate a tin-based PSC with an ETL-free structure and spiro-MeOTAD as the HTL. Similarly, our proposed effort will be based on SCAPS 1-D numerical simulation for the structure in [10] but with additional ETL layer based on three different metal oxides (ZnO , TiO_2 and SnO_2) and further emphasis on the transport layer thickness. Significantly, the effect of transport layer thickness towards the lead-free PSC parameters will be very useful to the solar cells research community, particularly those working on fabrication technique and process.

2. METHODS

The cross section of simulated planar n-i-p lead-free halide perovskite solar cells is shown in Fig. 1. In this structure, a transparent conducting oxide (TCO) is used as the front contact and it is followed by ETL. The methylammonium tin iodide ($CH_3NH_3SnI_3$) perovskite is the light absorber layer and spiro-MeOTAD will be applied as the HTL. Au is used as the metal back contact in this simulation. In the first phase of this work, we will validate our SCAPS 1-D simulation with the reported work by Liangsheng et al. [10], which is based on ETL-free structure. Note that, the authors in [10] adopted similar - to the proposed in this work - structure and materials. Material properties for ETL, HTL and $CH_3NH_3SnI_3$ perovskite absorber are extracted from [7, 10] and exhibited in Table 1 in which FTO , DOS_{CB} and DOS_{VB} denote fluorine-doped tin oxide, density of states for conduction band and density of states for valence band, respectively.

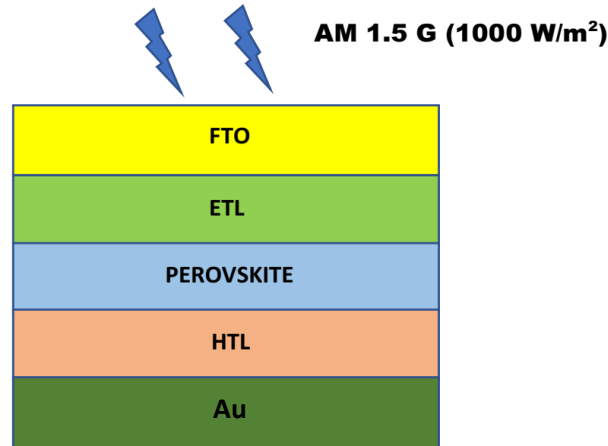


Fig. 1. Planar n-i-p lead-free PSC structure.

Table 1. Material properties for n-i-p lead-free PSC.

Properties	FTO	CH ₃ NH ₃ SnI ₃	Spiro-MeOTAD	SnO ₂	TiO ₂	ZnO
Thickness [nm]	500	400	200	80	80	80
Bandgap [eV]	4.3	1.3	3.1	3.6	3.3	3.2
Affinity [eV]	4.0	4.17	2.05	3.93	4.2	4.1
Dielectric Permittivity	9	8.2	3	8	10	8.1
DOS _{CB} [cm ⁻³]	2.2x10 ¹⁸	1x10 ¹⁸	2.2x10 ¹⁸	3.16x10 ¹⁸	2.5x10 ¹⁸	4.5x10 ¹⁸
DOS _{VB} [cm ⁻³]	1.8x10 ¹⁹	1x10 ¹⁸	1.8x10 ¹⁸	2.5x10 ¹⁹	1x10 ¹⁸	1x10 ¹⁸
μ _e [cm ² /Vs]	20	300	0.0002	15	0.1	15
μ _h [cm ² /Vs]	10	15	0.0002	0.1	0.1	1
Acceptor concentration [cm ⁻³]	0	3x10 ¹⁵	1x10 ¹⁸	0	0	0
Donor concentration [cm ⁻³]	2x10 ¹⁹	0	0	1x10 ¹⁹	1x10 ¹⁹	1x10 ¹⁹

Subsequently, our validated model will adopt three different inorganic metal oxide (ZnO, TiO₂ and SnO₂) as the ETL. In this second phase, the absorber thickness will be varied from 400 to 1500 nm. The purpose of this phase is to determine how the thickness of the absorber layer affects the solar cell performance for ETL-added structures.

In the third phase, the thickness of ETL is varied and the PSC performance parameters will be examined. The transport layers will be varied from 1 to 300 nm. Note that the other layers of PSC remain unchanged. For clarity, the energy level for each layer of this simulated PSC is shown in Fig. 2.

SCAPS 1-D is a one-dimensional solar cell software created by Marc Burgelman and his co-workers at the University of Gent [13]. In SCAPS 1-D simulation, three equations which comprise of Poisson equation (Eq. (1)) and continuity equations for electrons (Eqs. (2) and (3)) and holes (Eqs. (4) and (5)) are solved. Numerically, SCAPS 1-D solves for electrostatic potential, electron concentration and hole concentration in one dimension with respect to the position coordinate (x-coordinate in this case). The solar illumination model adopted in this work is internally generated by the software at AM 1.5 G (1000 Wm⁻²).

$$\frac{d^2\varphi(X)}{dX^2} = -\frac{\partial E}{\partial X} = -\frac{p}{\epsilon_s} = -\frac{q}{\epsilon_s} [p - n + N_D^+(X) - N_A^+(X) \pm N_{def}(X)] \quad (1)$$

$$\frac{\partial J_n}{\partial X} + G - U_n(n, p) = 0 \quad (2)$$

$$J_n = qn\mu_n E + qD_n \frac{\partial n}{\partial x} \tag{3}$$

$$-\frac{\partial J_p}{\partial x} + G - U_p(n, p) = 0 \tag{4}$$

$$J_p = qn\mu_p E + qD_p \frac{\partial p}{\partial x} \tag{5}$$

where φ is the electric potential, ϵ_s is the relative permittivity, q is the elementary charge, n is the electron density, p is the hole density, N_{D^+} is the density of ionized donors, N_{A^+} is the density of ionized acceptors, J_n is the electron current density, J_p is the hole current density, G is the electron-hole generation rate, U_n/U_p is the recombination rate, D_n is the diffusion coefficient of electrons, D_p is the diffusion coefficient of holes, μ_n is the electron mobility and μ_p is the hole mobility.

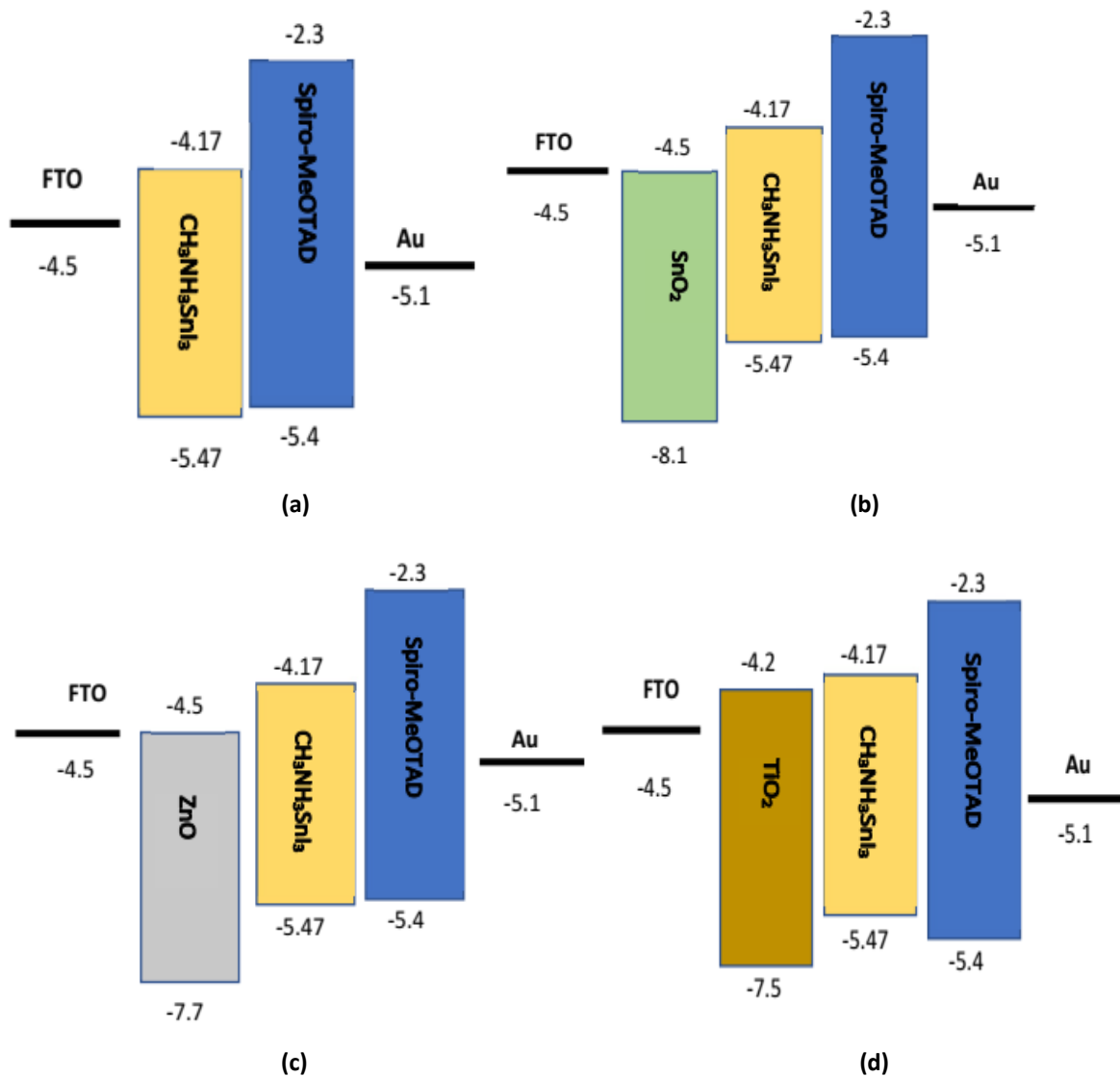


Fig. 2. Energy level diagram for each layer of the simulated PSC: a) ETL-free [10]; b) SnO₂ as the ETL; c) ZnO as the ETL; d) TiO₂ as the ETL.

3. RESULTS AND DISCUSSION

In the first part of this work, we have validated the SCAPS 1-D simulator by mimicking the ETL-free structure of [10], which is signified by the energy level diagram in Fig 2(a). The

inputs to the simulator are based on the data depicted in Table 1. Results of the obtained PSC parameters (V_{oc} , J_{sc} , FF and PCE) in our work and those of Liangsheng et al. [10] are given in Table 2, which shows that our simulated results are consistent with the simulated work by Liangsheng and his co-workers [10]. This indicates the accuracy of our SCAPS 1-D simulation technique, which can be further explored for another possible PSC configuration.

Table 2. Comparison between our simulated results and those of Liangsheng et al. [10].

Parameter	Current work	Liangsheng et. al. [10]
V_{oc} [V]	0.7332	0.7331
J_{sc} [mA/cm ²]	19.4362	19.3961
FF [%]	44.70	44.65
PCE [%]	6.37	6.35

In the second part of this work, the thickness of the methylammonium tin iodide perovskite absorber layer is varied from 400 to 1500 nm with other layers kept unchanged. Note that the thickness for both HTL and ETL remains constant at 80 nm. The simulated graphs for PSC parameters with respect to absorber thickness variation are shown in Fig. 3.

In general, it can be concluded that V_{oc} increases with the increment of absorber thickness for all metal oxides. The same phenomena can be recorded for the I_{sc} which shows proportional increment between 500 nm and 800 nm and the value remains constant above 900 nm. Factually, more charge carriers will be generated because of thicker absorber, which persistently provide more exposure to the sun. However, there is an optimum thickness which will not give significant effect to the current increment. Evidently, this is portrayed by the PCE figure which gives the optimum value at 900 nm for all metal oxides. Above this absorber thickness, no significant changes can be recorded for the PCE. The maximum point of PCE varies according to the ETL materials, which shows that SnO_2 produces the highest PCE of 8.10% as compared to ZnO of 8.05% and TiO_2 of 7.99%.

For comparison purposes, few published reports on Sn-based PSC have been adopted and the results are depicted in Table 3. Note that the structures are based on n-i-p configuration. Based on the data, it can be deduced that our simulated results are much lower compared to the established reports [11-13]. Theoretically, the major design parameters of PSC (V_{oc} , J_{sc} , FF and PCE) can be tuned according to various factors, which include the absorber thickness, layers' defect density value, materials for transport layers, bandgap variation, donor/acceptor concentration and operating temperature. Evidently, these factors have been firmly considered in [11-13] and they have successfully simulated the Sn-based PSC with improved performances. Note that our simulated structure is based on the established work by Liangsheng et al. [10] which yielded a PCE of 6.35 % for 400 nm $CH_3NH_3I_3$ absorber thickness non-ETL Sn-based PSC. Based on our presented results, the PCEs have been improved by absorber thickness optimization. It is worth to mention here that although our simulated PCEs are relatively lower, the basis of this proposed work is to investigate the effects of ETL thickness variation to the major design parameters of Sn-based PSC.

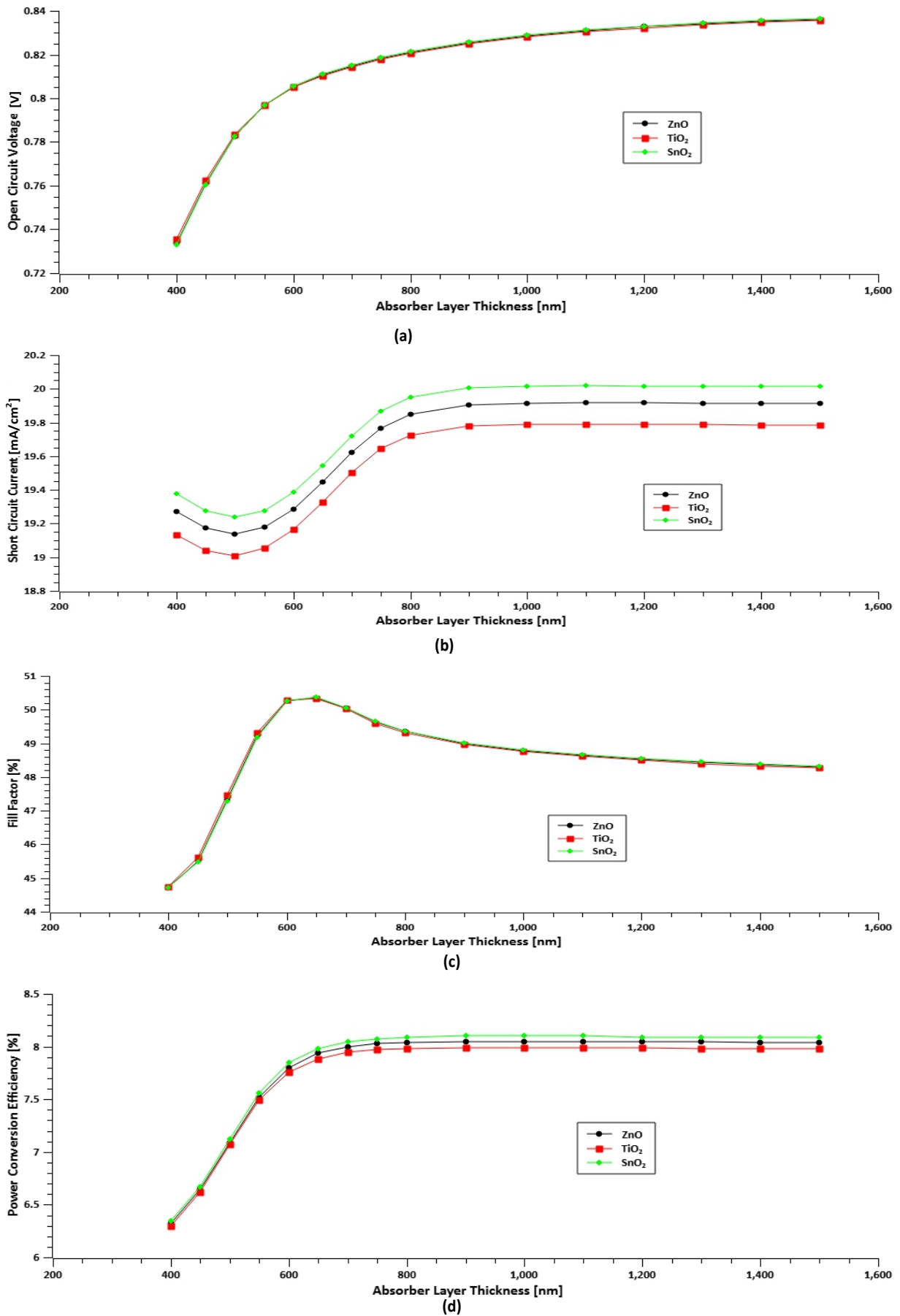


Fig. 3. Effect of absorber layer thickness on PSC parameters: a) V_{OC} ; b) J_{SC} ; c) FF; d) PCE.

Table 3. Parameters of the investigated PSCs compared to the state-of-the-art PSCs.

Solar cell structure	Parameter			
	V _{oc} [V]	J _{sc} [mA/cm ²]	FF [%]	PCE [%]
TCO/ZnO/CH ₃ NH ₃ I ₃ /CuI/Au [11]	1.1168	33.57	86.77	32.53
TCO/ZnO/CH ₃ NH ₃ I ₃ /Spiro-OMeTAD/Au [11]	1.1152	33.30	86.49	32.12
TCO/TiO ₂ /CH ₃ NH ₃ I ₃ /CuI/Au [11]	1.1169	33.60	89.03	33.41
TCO/TiO ₂ /CH ₃ NH ₃ I ₃ /Spiro-OMeTAD/Au [11]	1.1153	33.33	88.95	33.06
FTO/TiO ₂ /CH ₃ NH ₃ I ₃ /Cu ₂ O/Au [12]	0.66	42.70	69.82	18.36
FTO/ZnO NP/ CH ₃ NH ₃ I ₃ /CuSCN/Au [13]	0.89	32.8	79.65	23.51
FTO/ZnO NP/ CH ₃ NH ₃ I ₃ /CuSbS ₂ /Au [13]	0.86	32.68	77.31	21.74
FTO/ZnO NP/ CH ₃ NH ₃ I ₃ /CuI/Au [13]	0.95	32.41	70.96	22.06
FTO/ZnO NP/ CH ₃ NH ₃ I ₃ /NiO/Au [13]	0.77	32.05	77.83	19.27
FTO/ZnO NP/ CH ₃ NH ₃ I ₃ /P3HT/Au [13]	1.20	35.5	53.78	21
FTO/ZnO NP/ CH ₃ NH ₃ I ₃ /PeDOT PSS/Au [13]	0.92	32.43	69.98	20.89
FTO/ZnO NP/CH ₃ NH ₃ I ₃ /Spiro-OMeTAD/Au [13]	0.949	32.41	72.89	22.42
FTO/CH ₃ NH ₃ I ₃ /Spiro-OMeTAD/Au [10]	0.7331	19.39	44.65	6.35
FTO/SnO ₂ /CH ₃ NH ₃ I ₃ /Spiro-OMeTAD/Au [this work]	0.8312	20.01	48.66	8.10
FTO/TiO ₂ /CH ₃ NH ₃ I ₃ /Spiro-OMeTAD/Au [this work]	0.8249	19.78	48.97	7.99
FTO/ZnO/CH ₃ NH ₃ I ₃ /Spiro-OMeTAD/Au [this work]	0.8253	19.91	49.00	8.05

Subsequently, the effect of ETL thickness to the lead-free PSC is investigated. In this work, the ETL thickness has been varied up to 300 nm. Note that the HTL (spiro-MeOTAD) thickness kept unchanged at 80 nm throughout the simulation. The results are graphically presented in Fig. 4. It can be observed that the V_{OC} and FF are relatively constant for SnO₂ thickness span. In contrast, the V_{OC} is reduced with TiO₂ and ZnO thickness increment and vice versa for the FF. For I_{SC}, there is a very small reduction for SnO₂ as compared to ZnO and TiO₂, which has been observed to be significantly reduced. Importantly, it can be noted that the PCE for all ETL candidates have been reduced (ZnO by 0.99%; SnO₂ by 0.12%; TiO₂ by 0.63%) for ETL thickness increment from 80 nm to 300 nm.

Based on the presented figures, the increment of ETL thickness will certainly reduce the solar cell PCE. Apparently, this can be explained by realizing that higher values of ETL thickness will cause longer path of charge transportation. Eventually, it will increase the likelihood of carriers recombination and further reduce the generated photo current and hence, the PCE value.

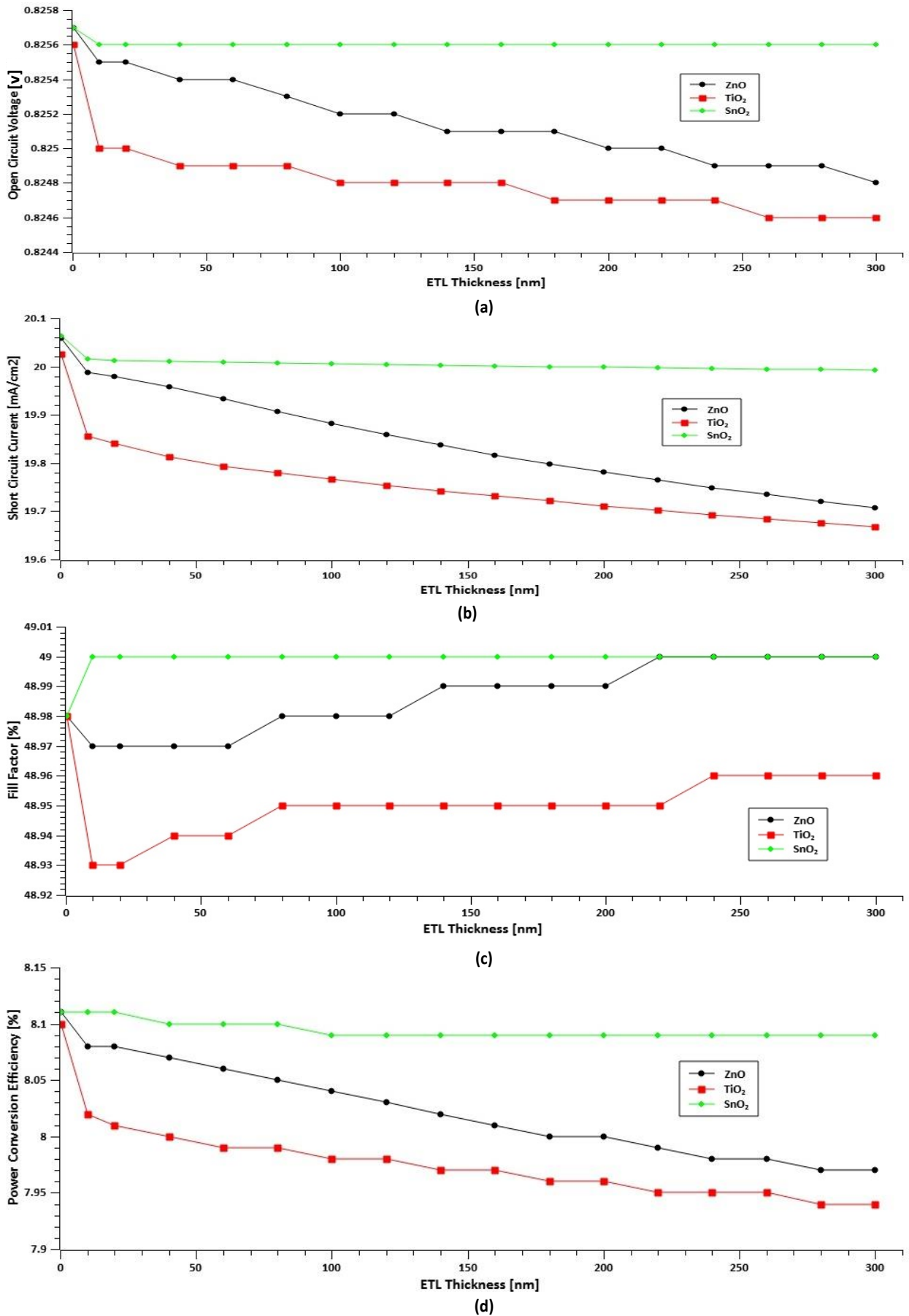


Fig. 4. Effect of ETL thickness on PSC parameters: a) V_{OC} ; b) J_{SC} ; c) FF; d) PCE.

4. CONCLUSIONS

This paper demonstrated that for planar n-i-p Sn-based PSC - with FTO/ETL/CH₃NH₃SnI₃/spiro-MeOTAD/Au configuration - SnO₂ as the ETL produced the highest PCE followed by ZnO and TiO₂. Initially, for SCAPS 1-D validation, comparisons were made with established reported work, which is based on ETL-free structures. We also demonstrated that for all ETL candidates, the optimum CH₃NH₃SnI₃ absorber thickness that produced the highest PCE is at 900 nm. Comparisons with previously published works on Sn-based PSC were made and feasible justifications were presented. Crucially, we had simulated for the first time, the effect of ETL thickness to the performance parameters of Sn-based PSC. The results showed that the PCE was reduced by 0.12% to 0.99% for all ETL candidates for ETL thickness increment from 80 nm to 300 nm. We strongly believe that the significant results reported here will surely assist future related works of PSC development and its research community.

Acknowledgement: Authors acknowledged Ministry of Higher Education of Malaysia for funding this research under Fundamental Research Grant Scheme (FRGS/1/2019/TK04/UTM/02/31). Special thanks to Dr Marc Burgelman from University of Gent, Belgium for the SCAPS 1-D software.

REFERENCES

- [1] W. Becquerel, "Photovoltaic effect in binary compounds," *The Journal of Chemical Physics*, vol. 5, pp. 1505-1514, 1960.
- [2] A. Kojima, K. Teshima, Y. Shirai, T. Miyasaka, "Organometal halide perovskites as visible light sensitizers for photovoltaic cells," *Journal of the American Chemical Society*, vol. 131, pp. 6050-6051, 2009.
- [3] National Renewable Energy Laboratory, *Best Research-Cell Efficiency Chart*, 2022. <<https://www.nrel.gov/pv/assets/pdfs/cell-pv-eff-emergingpv-rev220630.pdf>>
- [4] S. Jamal, A. Daud Khan, A. Daud Khan, "High performance perovskite solar cell based on efficient materials for electron and hole transport layers," *Optik*, vol. 218, no. 164787, 2020.
- [5] T. Ouslimane, L. Et-taya, L. Elmaimouni, A. Benami, "Impact of absorber layer thickness, defect density and operating temperature on the performance of MAPbI₃ solar cells based on ZnO electron transporting material," *Heliyon*, vol. 7, no. e06379, 2021.
- [6] F. Afri, A. Meftah, N. Sengouga, A. Meftah, "Electron and hole transport layers optimization by numerical simulation of a perovskite solar cell," *Solar Energy*, vol. 181, pp. 372-378, 2019.
- [7] M. Sazzadur Rahman, S. Miah, M. Wang Marma, T. Sabrina, "Simulation based investigation of inverted planar perovskite solar cell with all metal oxide inorganic transport layers," *Proceedings of International Conference of Electrical, Computer and Communication Engineering*, pp. 7-9, 2019.
- [8] S. Pachori, R. Agrawal, B. Lal Choudhary, A. Singh Verma, "An efficient and stable lead-free organic-inorganic tin iodide perovskite for photovoltaic device: progress and challenges," *Energy Reports*, vol. 8, pp. 5753-5763, 2022.
- [9] C. Devi, R. Mehra, "Device simulation of lead-free MASnI₃ solar cell with CuSbS₂ (copper antimony sulfide)," *Journal of Materials Science*, vol. 54, pp. 5615-5624, 2019.
- [10] H. Liangsheng, Z. Min, S. Yubao, M. Xinxia, W. Jiang, Z. Qunzhi, F. Zaiguo, L. Yihao, H. Guoyu, L. Tong, "Tin-based perovskite solar cells: Further improve the performance of the electron transport layer-free structure by device simulation," *Solar Energy*, vol. 230, pp. 345-354, 2021.

- [11] K. Fatema, M. Arefin, "Enhancing the efficiency of Pb-based and Sn-based perovskite solar cell by applying different ETL and HTL using SCAPS 1-D," *Optical Materials*, vol. 125, no. 112036, 2022.
- [12] P. Patel, "Device simulation of highly efficient eco-friendly $\text{CH}_3\text{NH}_3\text{SnI}_3$ perovskite solar cell," *Scientific Reports*, vol. 11, no. 3082, 2021.
- [13] P. Roy, Y. Raoui, A. Khare, "Design and simulation of efficient tin based perovskite solar cells through optimization of selective layers: theoretical insights," *Optical Materials*, vol. 125, no. 112057, 2022.
- [14] S. Rai, B. Pandey, A. Garg, D. Dwivedi, "Hole transporting layer optimization for an efficient lead-free double perovskite solar cell by numerical simulation," *Optical Materials*, vol. 121, no. 111645, 2021.
- [15] N. Singh, A. Agarwal, M. Agarwal, "Numerical simulation of highly efficient lead-free all-perovskite tandem solar cell," *Solar Energy*, vol. 208, pp. 399-410, 2020.
- [16] J. Madan, R. Pandey, R. Sharma, "Device simulation of 17.3% efficient lead-free all-perovskite tandem solar cell," *Solar Energy*, vol. 197, pp. 212-221, 2020.
- [17] M. Burgelman, K. Decock, S. Khelifi, A. Abass, "Advanced electrical simulation of thin film solar cells," *Thin Solid Films*, vol. 535, pp. 296-301, 2013.